Preprint of: Narożny M., Żakowski K., Darowicki K.: Application of Electrochemical Impedance Spectroscopy to evaluate cathodically protected coated steel in seawater. CONSTRUCTION AND BUILDING MATERIALS. Vol. 181 (2018), pp. 721-726. DOI: 10.1016/j.conbuildmat.2018.06.033

Application of Electrochemical Impedance Spectroscopy to evaluate cathodically protected coated steel in seawater

M. Narozny[1)], K. Zakowski[1)], K. Darowicki[1)]

[1)] Department of Electrochemistry, Corrosion and Materials Engineering, Chemical Faculty, Gdansk University of Technology, 11/12 Narutowicza St., 80-233, Gdansk, Poland

Corresponding author e-mail: michal.narozny@pg.gda.pl

Abstract:

Two types of organic coated carbon steel (S235JR2 grade) electrodes were exposed to artificial seawater environment. One prepared type was defect free while the other one had an intentionally introduced ϕ0,5 cm coating defect. Both kinds of samples were polarized during the exposure to four potentials corresponding to four different cathodic protection levels. Evolution of their EIS spectra is presented in this paper. Results obtained in the experiment indicate that protective organic coating condition could be estimated and monitored in time based on EIS investigations. If a sample is defected EIS allows a recognition of overprotected and unprotected sample. Distinguishing a fully protected sample from partially protected sample based on EIS was troublesome.

Keywords: Organic coatings; Cathodic Protection; Seawater; Electrochemical Impedance Spectroscopy; Steel.

1. Introduction

Organic coatings are the most often and commonly used anti-corrosion technique [1-2]. Coatings provide passive barrier against the aggressive environment. However, coatings provide protection as long as they remain intact and active pigments are not replenished [3-4]. On the other hand, cathodic protection (CP) system is capable of reducing corrosion rate even if a coating fails. CP is an electrochemical technique thus it's not capable of stopping corrosion completely but it significantly reduces its rate [5-6]. Organic coatings and CP are jointly used to provide a holistic anti corrosion protection [7]. Without a coating current demand of CP system could be so great that it might be technically impossible to implement. A proper coating system may reduce current demand by over 99 %. Even after years of operation coatings can reduce cathodic current demand by 70-80% or more [8]. However, it is important to remember that certain coatings are not compatible with CP systems. Therefore it remains a factor which has to be taken into account when a complex corrosion protection

system is designed [9]. A working CP system produces OH^- ions at the cathode increasing the alkalinity of the environment. There is always a risk that an ill-working CP system may cause coating deterioration and disbondment [10-12]. Especially if a critical potential is reached and water decomposition and hydrogen evolution occurs [13-15]. A cathodic protection system can rapidly increase coating deterioration if it has been not been properly supervised.

Modern CP rectifiers are often controlled by microcomputers. Unlike old manually adjustable units functionality of the modern rectifiers can be easily extended. CP rectifiers could be equipped with automatic on/off switcher, GPS time stamp, data logger and transmission unit, a watchdog, electric resistance corrosion coupon probe electrode, array of reference electrodes for stray current detection or other devices [16-21]. Due to the rapid electronic device development even Electrochemical Impedance Spectroscopy (EIS) module could be fit [22]. EIS is a technique capable of yielding information about impedance of the investigated system in the investigated frequency bandwidth. EIS data can be linked to the occurring electrochemical processes or physical properties of the investigated system [23-25].

In this paper an experiment involving EIS investigation of S235JR2 grade steel samples coated with organic coating under several cathodic protection conditions has been proposed. The coatings have been immersed in seawater for as long as 9 months. EIS data has been collected in order to verify its usefulness as a supplementary CP evaluation technique.

2. Materials and methods

A set of circular steel electrodes made of S235JR2 was manufactured. Composition of S235JR2 is presented in Tab. 1. Their radius equalled 6 cm and surface area 28,25 cm^2. Steel substrates and cable connectors were embedded in epoxy resin and insulated from environment.

Element Ultimate Tensile Strength	C [%]	Mn [%]	Si [%]	P [%]	S [%]	N [%]	UTS [N/mm2]
S235JR steel	0,17- 0,20	Max 1,3	-	0,045	0,045	0,009	360-490

Tab. 1 Composition and ultimate tensile strength of S235JR2 steel.

Specimen were sandblasted to the Sa3 NACE “white metal blast cleaning” surface roughness [26]. Substrates have been covered with a commercially available epoxy coating. According to the product specification the coating was designed to be applied as a single or multi-layer system. The coating was also confirmed to be CP compatible. Average coating thickness equalled 350 µm and its standard deviation 13 µm. Two sets of samples were prepared. One type of specimen was defect-free, the other one had a Φ0,5 cm holiday (Fig. 1).

Furthermore, weight loss coupons made of 100 cm^2 S235JR2 steel grade were manufactured and were exposed under the same conditions as the test specimens. They were prepared accordingly with EIS specimen.

Fig. 1 Samples after exposure. A defect-free sample (left) and a sample with Φ 0,5 cm holiday (right).

In accordance to European Standard EN 12473 "General principles of cathodic protection in sea water" four potentials corresponding to four different cathodic protection levels were chosen (Tab. 2)**Błąd! Nie można odnaleźć źródła odwołania.**. For every protection level a separate set of samples (no holiday/ Φ0,5 cm holiday) was prepared. During the entire exposure duration for every cathodic protection level a dedicated potentiostat was assigned to control electrochemical potential of specimen. Specimen were immersed in 50x20x30 cm tanks filled with 30 l of artificial seawater. Artificial sea water composition was prepared in agreement with ASTM D1141-98 standard. Details are presented in Tab. 3 [27]. Salts with content lower than KBr were not used.

Cathodic protection level	Potential vs $Zn/ZnSO_4$ (saturated) [mV]	Potential vs Ag|AgCl|Seawater [mV]
No protection	Free corrosion potential On average +363	Free corrosion potential, On average -675
Under protection	+288 mV	-750
Full protection	+88 mV	-950
Overprotection	-162 mV	-1200

Tab. 2 Cathodic protection levels and potentials of specimen.

Anodes – auxiliary electrodes made of 20x15 cm mixed metal oxide covered titanium mesh were utilized. Saturated $Zn|ZnSO_4$ reference electrodes were chosen and placed as close as possible to the specimen in order to reduce IR drop. In order to ensure a good cathodic current distribution anodes were located as far away from the working electrodes as possible. During the exposure weigh loss coupons and samples were electrically shortened. For EIS experiments Ag|AgCl|Seawater reference electrode was used. Every sample was then electrically disconnected and evaluated separately.

Salt	NaCl	$MgCl_2$	Na_2SO_4	$CaCl_2$	KCl	$NaHCO_3$	KBr
Concentration [g/dm^3]	24,53	5,20	4,09	1,16	0,695	0,201	0,101

Tab. 3 Artificial seawater composition according to ASTM D1141-98.

Every few days Electrochemical Impedance Spectroscopy experiments were performed. In the beginning of the exposure intervals between experiments were short: ranging from 2 to 7 days. Once specimen condition stabilized measurements were taken less often – and intervals increased from 7 to 30 days. Perturbation amplitude equalled 15 mV and frequency bandwidth ranged from 0,05 Hz to 10 kHz. All tests were carried out using Gamry 1000 potentiostat.

3. Results and discussion

Long term exposure of coated specimen were performed in order to review applicability of EIS to investigate changes of cathodically protected systems in time. Specimen without a holiday were treated as a reference samples. Differences between samples without coating disruptions and intentionally defected samples and their time evolution under four CP protection levels regimes were anticipated to be observed.

Defect free specimen without CP during the experiment exhibited a straight-like line in their Bode spectrum (Fig. 2). Phase angle was very close to 90^o in the entire frequency range. A slight shift towards lower phase angles was observed in the low frequency range only, approaching a DC limit. A capacitive nature of the response suggests that the coating remains intact during entire exposure. Positive phase angle shift at the lowest frequencies indicates slow coating deterioration. Its character became more resistive. Impedance modulus at low frequencies remained higher than 10^9 Ω. If a surface area of the specimen is taken into account it translates to approximately $2{,}8 \cdot 10^{10}$ Ωcm^2. The impedance modulus and phase angle measured were characteristic for an unbroken, intact and fully protective coating (2).

Unlike in the case of the unprotected sample, the other specimen show indications of coating deterioration. It is more than likely that the cathodic protection accelerates coating deterioration. Characteristic spectra evolution of the fully coated specimen were observed for all samples with any degree of cathodic protection (Fig. 3-5). In the first spectrum taken (at the beginning of the experiment) impedance modulus forms an almost straight line. Phase shift was lower than -40^0 even at the lowest frequencies. The coating had a capacitive character. During the exposure an impedance modulus plateau had formed. Once the plateau was observed a distinctive phase shift became visible. Impedance of the system had a 0^o phase angle at the lowest frequencies and -90^o at higher frequencies. It indicated that coating nature had changed from purely capacitive (an intact coating) to resistive. When time passed the phase shift from 0^o to 90^o started occurring at higher and higher frequencies. The impedance modulus plateau value decreased. Plateau bandwidth was greater too, as the phase shift 'moved' towards higher frequencies. After the exposure the CP protected samples still exhibited some degree of protection.

Equivalent circuits with either one or two time constants fitted measured EIS spectra. Values of chi squared (X^2) which is a measure describing discrepancies between measured values and a model under investigation are presented for every figure which involves EIS model fitting. A model with two time constants was chosen for spectra which showed an indication of a second semicircle formation. Evolution of coating resistance is presented in Fig. 6. After quick initial breakdown all of the coatings reached a resistance plateau. Calculated coating capacity is presented in Fig. 7. Initial capacity and resistance of all coatings is almost the same – they have been applied in the same manner and had a similar thickness. All of them quickly increased their capacity due to water uptake. Then coating capacity did not increase any further and it remained stable for the entire duration of the experiment. The under protected sample exhibited impedance lower than 10^6 Ωcm^2 – a border line value for a protective coating.

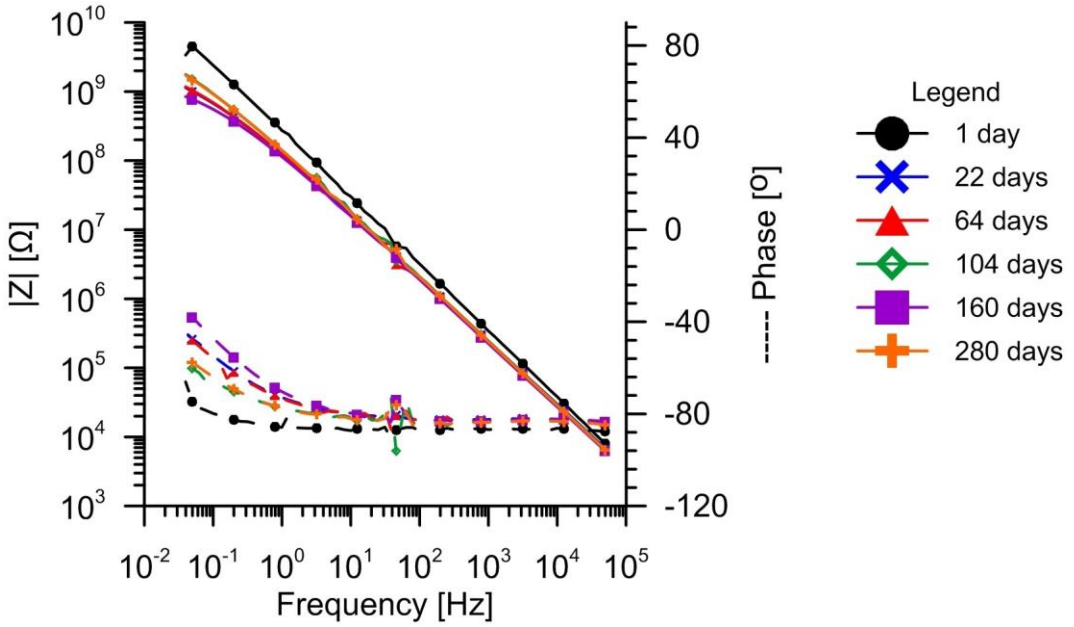

Fig. 2 Exemplary EIS Bode plots of CP unprotected defect-free organic coated specimen in time. To clarify the chart not every obtained plot is presented.

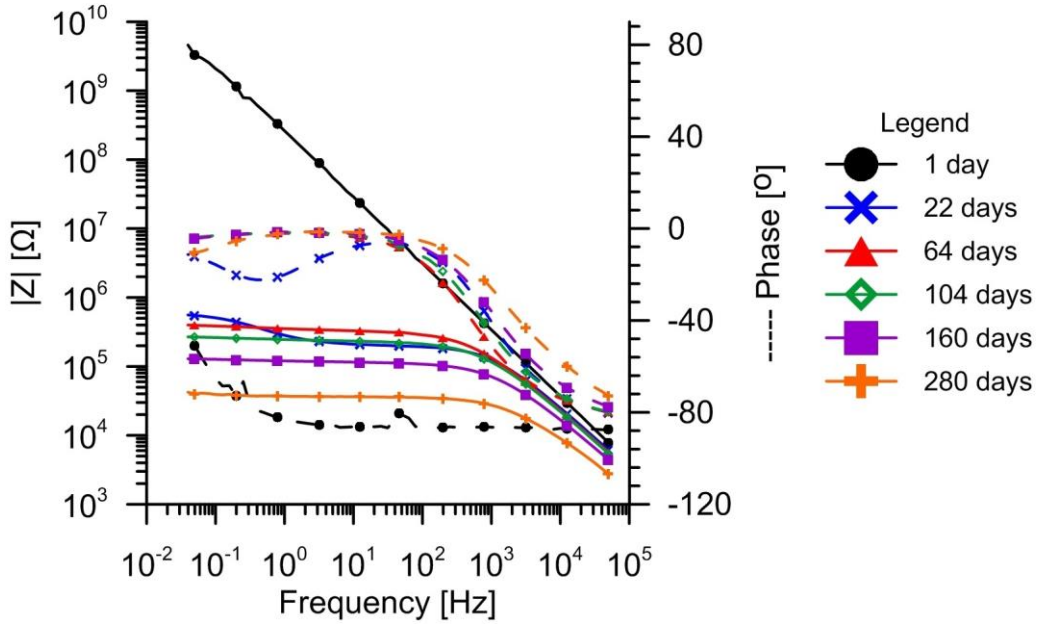

126

127 Fig. 3 Exemplary EIS Bode plots of CP under protected defect-free organic coated specimen in time. To
128 clarify the chart not every obtained plot is presented.

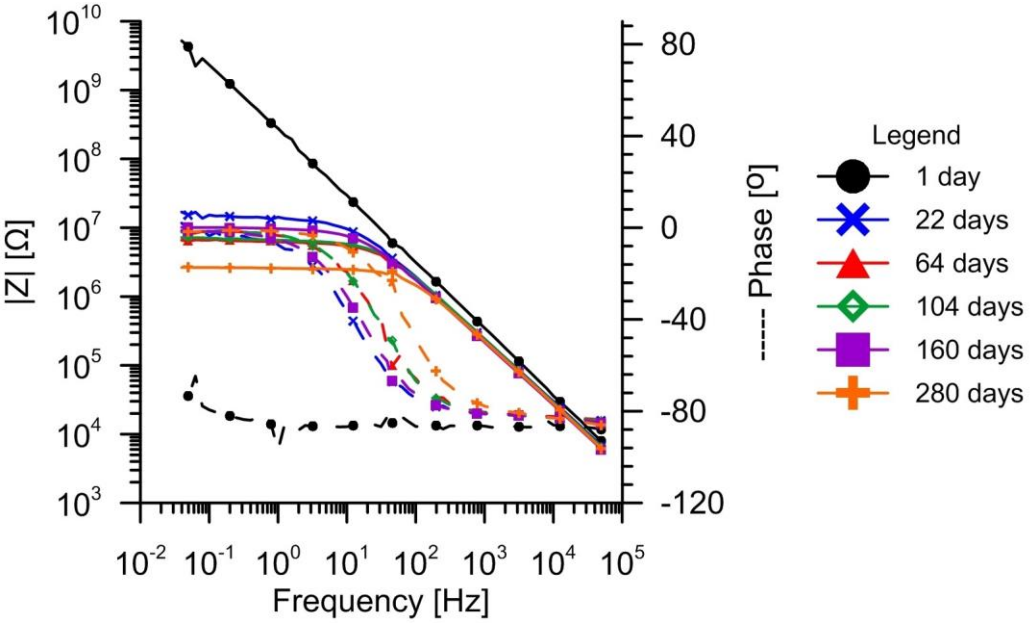

129

130 Fig. 4 Exemplary EIS Bode plots of CP fully-protected defect-free organic coated specimen in time. To
131 clarify the chart not every obtained plot is presented.

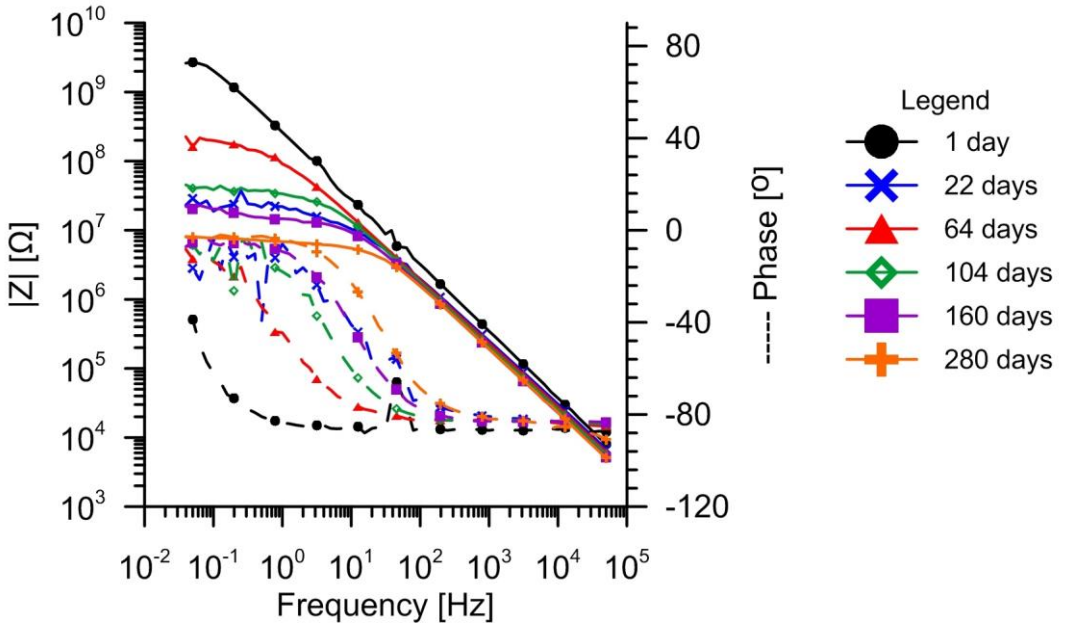

132

133 Fig. 5 Exemplary EIS Bode plots of CP overprotected defect-free organic coated specimen in time. To
134 clarify the chart not every obtained plot is presented.

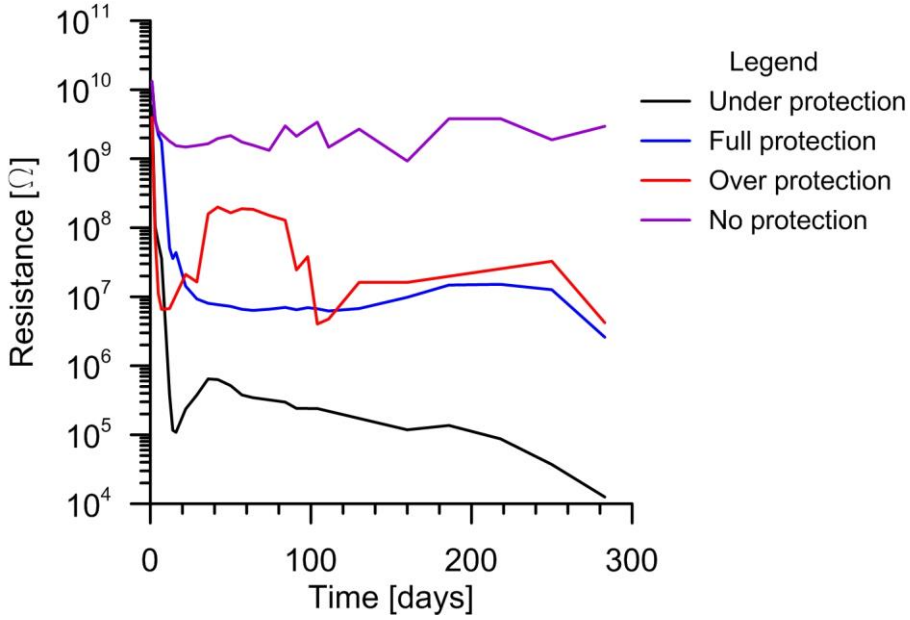

135

136 Fig. 6 Coating resistance vs time plot based on equivalent circuit model fit to the measured EIS spectra.
137 Chi squared (X2) – goodness of fit values ranged from $3{,}45 \cdot 10^{-4}$ to $1{,}04 \cdot 10^{-2}$.

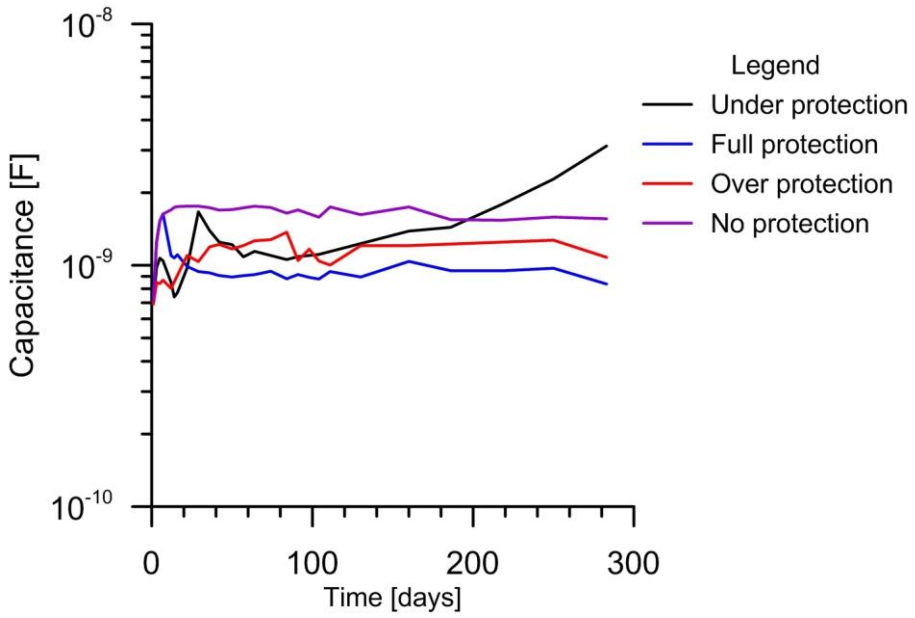

Fig. 7 Coating capacity vs time plot based on equivalent circuit model fit to the measured EIS spectra. Chi squared (X2) – goodness of fit values ranged from $3{,}45 \cdot 10^{-4}$ to $1{,}04 \cdot 10^{-2}$.

Spectra of an unprotected organic coated sample with a ϕ0,5 cm holiday are presented in Fig. 8. All of the spectra resemble a one time-constant system. A distinctive phase angle peak is visible, initially at approximately $2 \cdot 10^{1}$ Hz. The peak is shifted in time towards lower frequencies down to 1 Hz. However, it must be noted that there are two reactions occurring simultaneously – iron oxidation and oxygen reduction which cannot be distinguished with EIS.

Spectra of an under protected and fully protected organic coated sample with a ϕ0,5 cm holiday are presented in Fig. 9 and Fig. 10. Both of these cases are described together because their similarities can be immediately noticed. Initially, on a 1st day of exposure a phase peak is visible at frequency of 10 Hz (Fig. 9) and 100 Hz (Fig. 10). As time passed their phase angle flattened. At low and medium frequency bandwidth the response of the system became resistive (0° phase angle) and at higher frequencies it changed became more capacitive. Impedance modulus plateau appeared when phase angle approached zero at low and medium frequencies. It could be attributed to coating deterioration. Rising alkalinity of the environment due to oxygen reduction and increase of OH^- content might be the cause of this phenomenon. Accurate model fit to those EIS cases is troublesome due to the overlapping time constants. Flat and elongated Nyquist spectra for under protected and fully protected specimen are presented in Fig. 11.

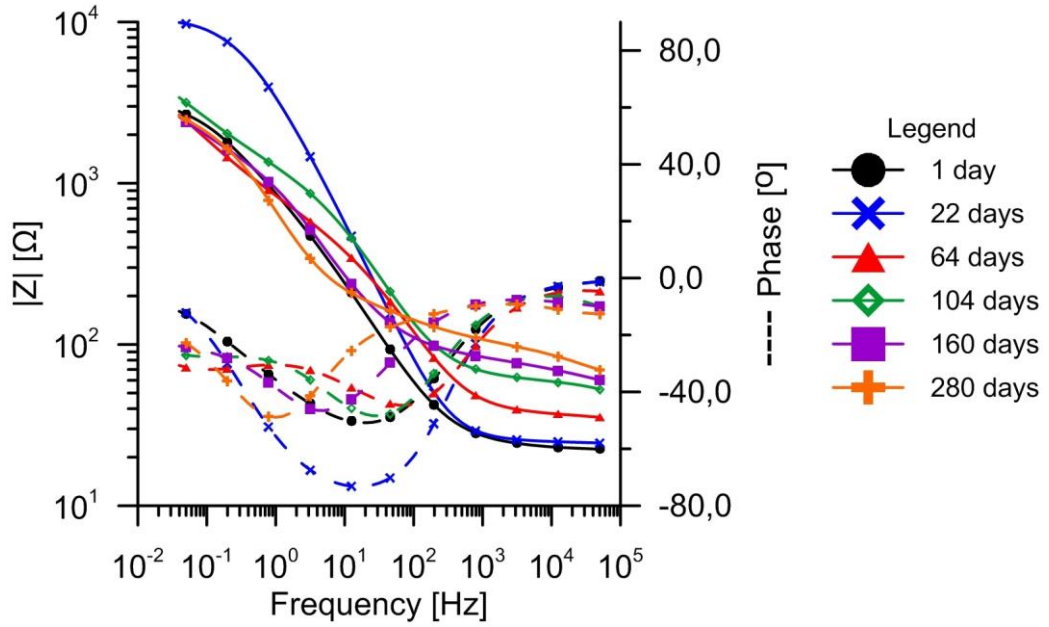

157

158 Fig. 8 Exemplary EIS Bode plots of CP unprotected organic coated specimen with a ϕ0,5 cm defect, in

159 time. To clarify the chart not every obtained plot is presented.

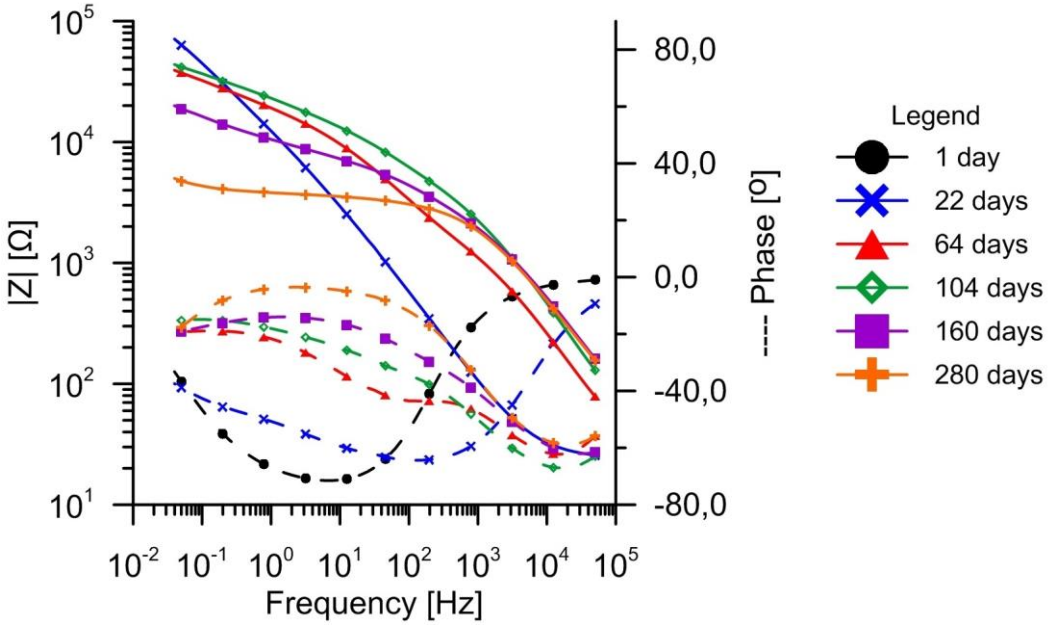

160

161 Fig. 9 Exemplary EIS Bode plots of CP under protected organic coated specimen with a ϕ0,5 cm defect,

162 in time. To clarify the chart not every obtained plot is presented.

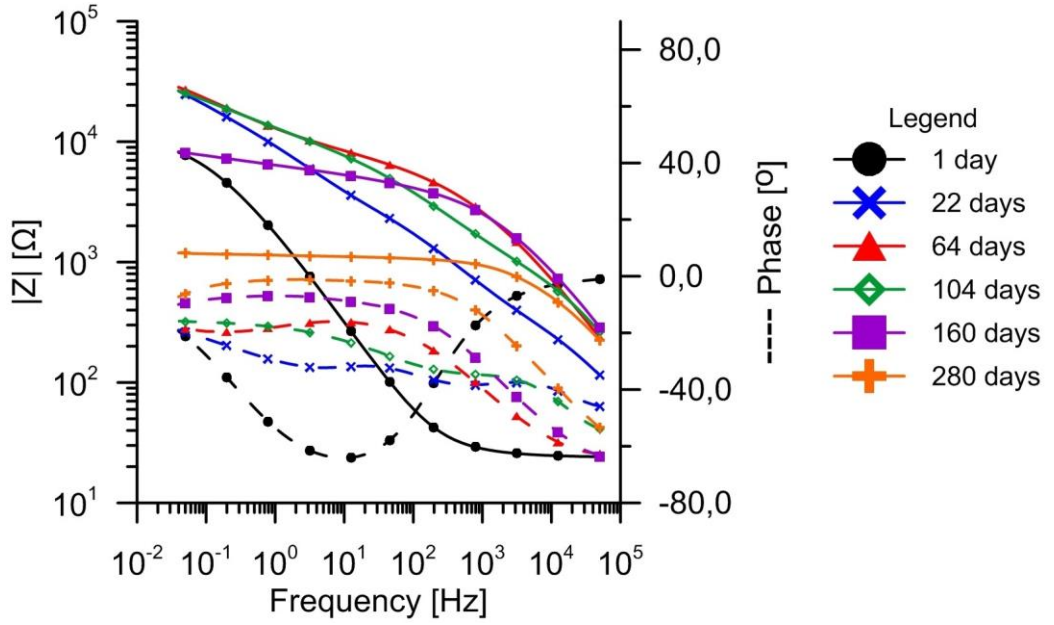

Fig. 10 Exemplary EIS Bode plots of CP fully protected organic coated specimen with a ϕ0,5 cm defect, in time. To clarify the chart not every obtained plot is presented.

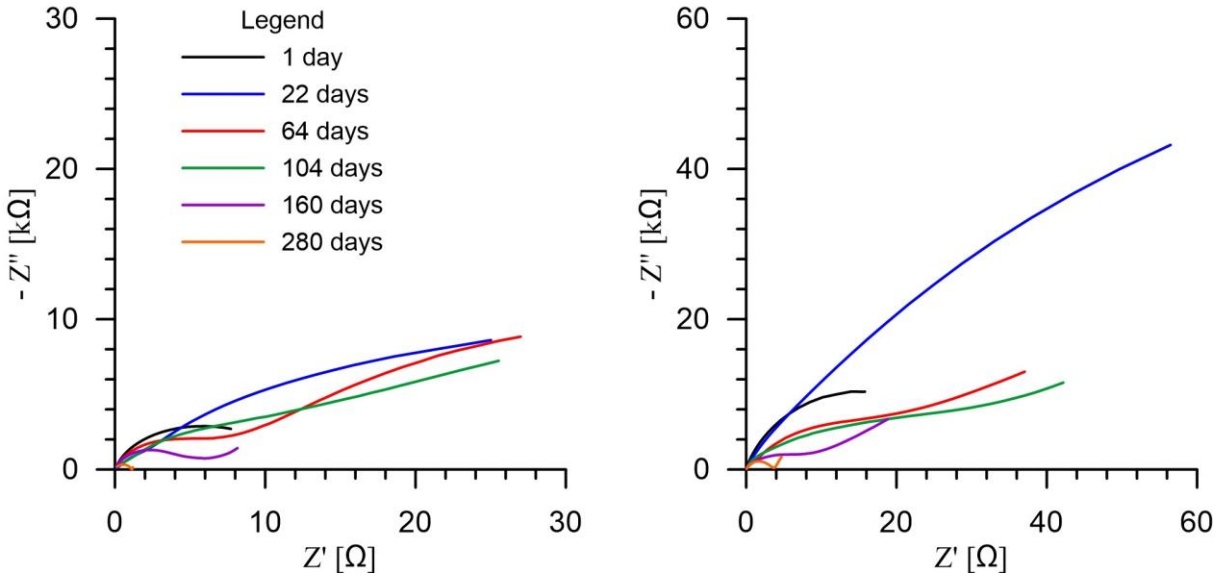

Fig. 11 Exemplary EIS Nyquist plots of CP under protected (left) and fully protected (right) organic coated specimen with a ϕ0,5 cm defect, in time. To clarify the chart no every obtained plot is presented.

Bode phase spectra of overprotected sample with a coating have a distinct peak (Fig. 12). Initially the peak appeared at approximately 10^2 Hz. Naturally overprotection (sample's potential of -1200 mV vs Ag|AgCl|seawater) involves occurrence of a fast reaction – water decomposition. In time the phase angle peak shifted towards lower frequencies, up to approximately 1 Hz. This phenomena could be

linked to the calcareous sediment layer evolution. Expanding calcareous layer reduces the active surface and the reaction eventually slows down. The phase peak is shifted towards lower frequencies. Unlike other specimen the impedance modulus spectra is shifted up in time. A new high frequency phase shift became more distinct later on. In a Nyquist plot it is visible as part of a second semicircle (Fig. 12). Its appearance can be most likely linked to the calcareous layer. It proves that the sediments reduce the reaction rate as the overall impedance modulus is increased. In case of the unprotected sample there is no distinct shift of the impedance modulus (with an expectation of the initial increase due to corrosion products formation). It can be assumed that the system response in the investigated frequency range is associated with water decomposition reaction and evolution of calcareous layer. In order to determine the evolution of polarisation resistance and calcareous layer resistance equivalent circuit model was fitted to the experimental data. Those quantities are presented in Fig. 13. The fact that sediment layer resistance increased in time proved its development and reduction of reactive surface area. As a result rate of water decomposition reaction declined and fitted polarisation resistance increased.

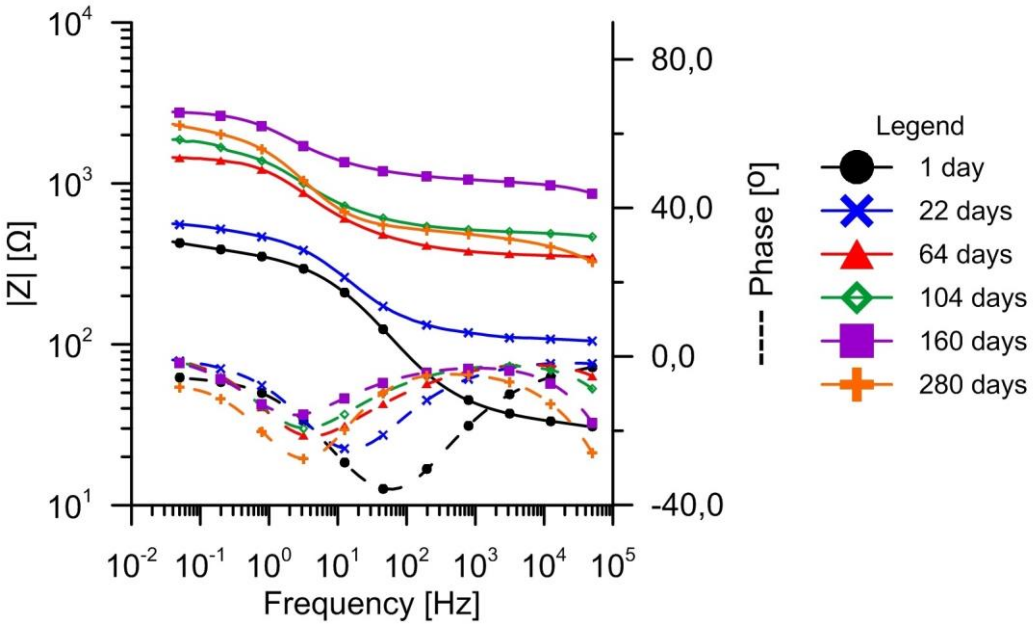

Fig. 12 Exemplary EIS Bode plots of CP overprotected organic coated specimen with a ϕ0,5 cm defect, in time. To clarify the chart not every obtained plot is presented.

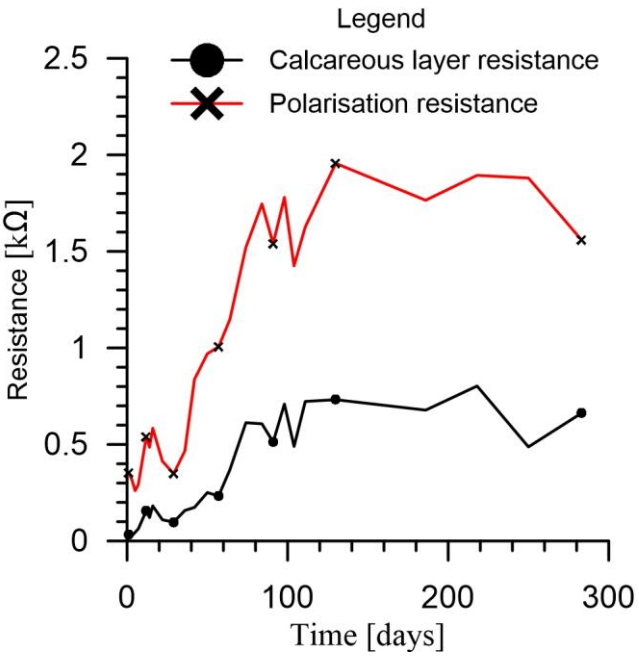

Fig. 13. Plot of polarisation resistance and calcareous layer resistance in time based on equivalent circuit model fit to the measured EIS spectra. Overprotected ϕ0,5 cm defected coating specimen. Chi squared (X2) – goodness of fit values ranged from $2{,}13 \cdot 10^{-5}$ to $7{,}45 \cdot 10^{-3}$.

Corrosion rates determined from weight loss coupons for unprotected, under protected, fully protected and overprotected were as follows: 0,073 mm/year, 0,007 mm/year, 0,003 mm/year, 0,002 mm/year. Obtained corrosion rates and their relative relations are reasonable and in accordance with values reported in literature for corresponding cathodic protection degrees.

4. Conclusions

Long term exposures of defect-free and ϕ0,5 cm defected epoxy coated specimen in four different cathodic protection conditions in artificial seawater were performed. Exposures lasted for over 9 months. Time evolution of spectra of investigated coatings was recorded.

An evolution of EIS spectra of a defect-free sample in all four CP conditions was similar and was characteristic for a deteriorating coating. However the coating deterioration with any degree of cathodic protection underwent quicker than in conditions without cathodic polarization. A CP unprotected coating retained its protective properties for the entire experiment without any major signs of a coating failure. Protective organic coating condition could be estimated and monitored in time based on EIS investigations.

Both overprotected and unprotected samples with a ϕ0,5 cm defect had a characteristic impedance spectra in the investigated frequency range. Their time evolution was described. If a sample is defected EIS allows a recognition of overprotected and unprotected sample.

Under protected and fully protected samples have similar spectra. Their evolution in time is also akin, same features are observed in their spectra and they evolve in the same pattern. However, the spectra evolution of a fully protected sample is significantly quicker. Distinguishing a fully protected sample from under protected sample based on EIS only is troublesome.

EIS is capable of providing additional information complementary to ordinary current and potential measurements. Based on the laboratory experiments a test electrode could be applicable as an additional information source of coating's sample condition. However the EIS data is troublesome to be analysed in situ. Data could be easily transferred from multiple measurement units and stored/transferred for analysis.

5. Acknowledgements

The contribution has been realized as a part of the grant 2012/05/N/ST8/02899 financed by the National Science Centre Poland.

6. References

1. Z. W. Wicks Jr., F. N. Jones, S. P. Pappas, D. A. Wicks. Organic Coatings: Science and Technology. s.l. John Wiley & Sons, 2007.

2. P. A. Sørensen, S. Kiil , K. Dam-Johansen, C. E. Weinell, Anticorrosive coatings: a review, J. Coat. Technol. Res. 6 (2009) 135-176.

3. M. Zubielewicz, W. Gnot, Mechanisms of non-toxic anticorrosive pigments in organic waterborne coatings, Prog. Org. Coat. 49 (2004) 359-371.

4. G. Williams, H.N. McMurray, M. J. Loveridge, Inhibition of corrosion-driven organic coating disbondment on galvanised steel by smart release group II and Zn(II)-exchanged bentonite pigments, Electrochim. Acta. 55 (2010) 1740-1748.

5. V. Ashworth, C.J.L. Booker. Cathodic protection: Theory and practice, John Wiley and Sons, New York, 1986.

6. Seong-Jong Kim, Masazumi Okido, Kyung-Man Moon, An electrochemical study of cathodic protection of steel used for marine structures, Korean J. Chem. Eng. 20 (2003) 560-565.

7. F. Gan, Z. W. Sun, G. Sabde, D. T. Chin, Cathodic Protection to Mitigate External Corrosion of Underground Steel Pipe Beneath Disbonded Coating, Corros. Eng. 50 (1994) 804-816.

8. K. Zakowski, Studying the effectiveness of a modernized cathodic protection system for an offshore platform, Anti-Corros. Method. M. 58 (2011) 167-172.

9. L. Martinez, L. V. Žulj, F. Kapor, Disbonding of underwater-cured epoxy coating caused by cathodic protection current, Corr. Sci. 51 (2009) 2253-2258.

10. Y. R. Yoo, H. H. Cho, S. Take, J. G. Kim, Y. S. Kim, Influence of cathodic protection on the lifetime extension of painted steel structures, Met. Mater. Int. 12 (2006) 255-261.

11. E. L. Koehler, The Mechanism of Cathodic Disbondment of Protective Organic Coatings—Aqueous Displacement at Elevated pH, Corr. Sci. 40 (1984) 5-8.

12. T. Kamimura, H. Kishikawa, Mechanism of Cathodic Disbonding of Three-Layer Polyethylene-Coated Steel Pipe, Corr. Sci. 54 (1998) 979-987.

13. C.F. Barth, A. R. Troiano, Cathodic Protection and Hydrogen in Stress Corrosion Cracking, Corrosion 28 (1972) 259-263.

14. L.H. Wolfe, C.C. Burnette, M.W. Joosten, Hydrogen embrittlement of cathodically protected subsea bolting alloys, Mater. Performance 32 (1993).

15. D, Festy, Cathodic Protection of Steel in Deep Sea: Hydrogen Embrittlement Risk and Cathodic Protection Criteria, Corrosion 2001, Conference materials.

16. R. W. Bosch, J. Hubrecht, W. F. Bogaerts, B. C. Syrett, Electrochemical Frequency Modulation: A New Electrochemical Technique for Online Corrosion Monitoring, Corr. Sci. 57(2001) 60-70.

17. C. Andrade, C. Alonso, Corrosion rate monitoring in the laboratory and on-site, Constr. Build. Mater. 10 (1996) 315-328.

18. J. P. Broomfielda, K. Davies, K. Hladky, The use of permanent corrosion monitoring in new and existing reinforced concrete structures, Cement Concrete Comp. 24 (2002) 27-34.

19. K. Zakowski, W. Sokolski, 24-hour characteristic of interaction on pipelines of stray currents leaking from tram tractions, Corr. Sci. 41 (1999) 2099-2111.

20. K. Żakowski, K. Darowicki, Methods of Evaluation of the Corrosion Hazard Caused by Stray Currents to Metal Structures Containing Aggressive Media, Pol. J. Environ. Stud. 9 (2000) 237-241.

21. K. Zakowski, K. Darowicki, Diagnosis of Reference Electrodes in Cathodic Protection Systems by Electrochemical Impedance Spectroscopy, Corros. Rev. 20 (2011) 391-402.

22. Guofu Qiao, Jinping Oua, Corrosion monitoring of reinforcing steel in cement mortar by EIS and ENA, Electrochim Acta 52 (2007) 8008-819.

23. M. Szocinski, K. Darowicki, Local impedance spectra of organic coatings, Polym. Degrad. Stabil. 98 (2013) 261-265.

24. S. Krakowiak, K. Darowicki, Inspection of rubber linings operating in flue gas desulphurisation units, Prog. Org. Coat. 46 (2003) 211-215.

25. K. Darowicki, P. Slepski, M. Szocinski, Application of the dynamic EIS to investigation of transport within organic coatings, Prog. Org. Coat. 52 (2005) 306-310.

26. NACE International, NACE No. 2/SSPC-SP 10 White Metal Blast Cleaning.

27. ASTM International. ASTM D1141 - 98 Standard Practice for the Preparation of Substitute Ocean Water, 2013.